Proceedings of the 12th International Conference on
Aluminium Alloys, September 5-9, 2010, Yokohama, Japan

pp. 727-732

On the Development of a Cold Cracking Criterion for DC-Casting of High Strength Aluminum Alloys

Mehdi Lalpoor[1], Dmitry G. Eskin[1,2], Laurens Katgerman[2]
[1] Materials innovation institute, Mekelweg 2, 2628 CD Delft, The Netherlands
[2] Delft University of Technology, Department of Materials Science and Engineering, Mekelweg 2, Delft, 2628 CD, The Netherlands

Direct Chill casting has been the mainstream of aluminum industry mainly due to its robust nature and high productivity. The casting problems however still affect the final quality of ingots. Large residual thermal stresses formed during casting at different locations of ingots and their sudden release on cast imperfections result in a catastrophic phenomenon called cold cracking. Residual thermal stresses may be troublesome especially below some critical temperatures where as-cast high strength aluminum alloys become extremely brittle. Thus, development of a criterion that predicts the onset of catastrophic failure would be of great benefit to the aluminum industry. This might be achieved in principle by applying the constitutive parameters as well as plane strain fracture toughness of a typical 7*xxx* series aluminum alloy in the genuine as-cast condition to thermo-mechanical simulations. Current research work presents the results of thermomechanical simulations on an AA7050 alloy. Contour maps of the residual thermal stresses and the consequent critical crack sizes reveal the locations and the stages where DC-cast billets are more prone to catastrophic failure. For round billets in the steady state regime, the critical locations appear to be the water impingement zone and the center of the billet.

Keywords: *DC-casting, Aluminum Alloys, Thermal Stress, Thermomechanical Simulations, Cold Cracking.*

1. Introduction

In spite of all technical improvements and developments in aluminum industry, ingots of high strength aluminum alloys still suffer from cracking and failure. The cracking may occur above solidus temperature when the major fraction of inter-dendritic spaces is covered by low melting point nonequilibrium eutectics and result in hot cracks [1]. It can also occur below solidus or at temperatures near room temperature where the material is extremely brittle, and lead to cold cracking [2]. It is not well understood whether cold cracks are the hot cracks that catastrophically propagate when reaching the critical length or they just occur when the elastic strain energy of the system releases abruptly on voids or brittle intermetallics. Therefore separate criteria for hot [3-6] and cold cracking [7-10] have been established. Criteria developed on cold cracking can be classified in two groups: experiment based criteria [7,8] and computer simulation based criteria [9,10]. Experimentally derived criteria have been based on the results of numerous cast trials under various casting conditions and ingot geometries. Livanov [7] e.g., noticed that to prevent hot cracks in slabs the cast speed should be lowered while he advised higher cast speeds to avoid cold cracks. Experimentally derived equations and graphs could eventually indicate the proper cast speed for the corresponding slab thickness, although casting of slabs thicker than a certain value appeared not to be feasible (probably due to the mold design available at that time). Computer simulation criteria on the other hand are more physically based and deal with the fracture mechanics concepts. According to the fracture mechanics, catastrophic failure occurs when a crack or flaw reaches a critical length in the presence of a tensile stress field. Normal stress values can be obtained through thermomechanical simulation of the DC casting process, and plane strain fracture toughness (K_{Ic}) values may be measured experimentally for the alloy under consideration. By application of fracture mechanics, the critical crack size leading to catastrophic failure can be calculated with right selection of the crack

geometry [9,10]. Results may be more realistic provided that the constitutive parameters as well as the K_{Ic} values are obtained from the material in the genuine as-cast condition [11,12]. In the present article, the results of thermomechanical simulations for an AA7050 alloy are reported. Using the computer simulated values of the maximum principal stress and application of K_{Ic} values from room temperature to 200°C, the critical crack sizes were calculated for the billets cast at two different speeds and the contour maps are presented.

2. Presentation of the model

ALSIM5 was used for the computation of temperature profile and stress/strain fields in the round AA7050 billet. The description of the model can be found elsewhere [13-15]. Geometry of the setup consisted of hot top, mold, water jet, bottom block, and the cast domain. New elements with the size of 0.75 mm are added to the geometry at the casting speed to simulate the continuous casting conditions. So during casting the bottom block moves downwards while new elements are added to the system, and the mold, hot top and molten metal preserve their initial position. Due to axial symmetry, only half of the billet is considered. Time dependent thermal boundary conditions are defined to account for filling time, the air gap formation between the billet and the bottom block as well as at the billet surface, and for different heat extraction in different parts of the casting system [16]. The process parameters are mentioned in Table 1.

Table1. Description of casting process parameters. Second values correspond to the billet cast at 2 mm/s.

Process parameter	Value
Ingot diameter (mm)	200
Final length of the billet (mm)	380 and 400
Casting speed (mm/s)	1 and 2
Melt temperature (ºC)	680
Water flow rate (l/min)	80, 200
Water temperature (ºC)	15
Start temperature of bottom block (ºC)	20

Thermal as well as fluid properties of the alloy were gained from the thermodynamics database JMat-Pro provided by Corus-Netherlands (IJmuiden). The temperature dependence of the coefficient of thermal expansion, specific heat, heat conductivity, fraction solid, density and kinematic viscosity were extracted and embedded in the model. The solidification range as well as the liquidus and the non-equilibrium solidus were determined using DSC tests. Tensile mechanical properties and constitutive parameters of as-cast 7050 samples were measured by authors in a Gleeble-1500 thermomechanical simulator and the details are described elsewhere [11]. K_{Ic} values were also measured by authors in the as-cast condition from room temperature to 200°C and the results may be found in [12]. A new module was introduced to ALSIM5 by means of which critical crack sizes could be calculated for the desired crack type and geometry based on the given K_{Ic} values and the maximum principal stress component.

3. Results and discussion

Casting simulation was performed for 380 seconds (casting length of 380 mm at 1 mm/s) to make sure that the steady-state conditions are gained and stress analysis can be done. After this moment, the stresses remained more or less unchanged until changes in the thermal boundary conditions were applied or casting ceased. As can be seen in Fig. 1a, the lower part of the billet has reached temperatures below 80 ºC. Figs. 1(b) through (d) show the contour maps of the normal residual thermal stresses generated under steady-state casting conditions. As can be seen, the residual radial

stresses displayed in the lower part of the billet (on the top of the bottom block) are compressive which turn to tensile as we move in the positive "y" direction. Along the radial axis (x-axis), radial stress diminishes from 71 MPa to 3 MPa as we move towards the surface. Similar trend is observed for the circumferential stress, but it turns to compressive in the vicinity of the surface (71 MPa in the center, and –86 MPa at the surface; Fig. 1c). Contour map of the axial stress (along "y" axis) follows the same trend in the lower part of the billet, i.e. tensile stresses in the center and compressive stresses at the surface. This, changes in the upper part of the billet where we see compressive stresses below the high temperature zone of the billet and tensile stresses around the water impingement area (Fig. 1d). It is important to note that the circumferential stress at the surface passes through a transition from tensile to compressive as soon as the surface leaves the water impingement zone (WIZ). The tensile stresses in the WIZ reach the highest value (73 MPa) among the stresses formed in the billet.

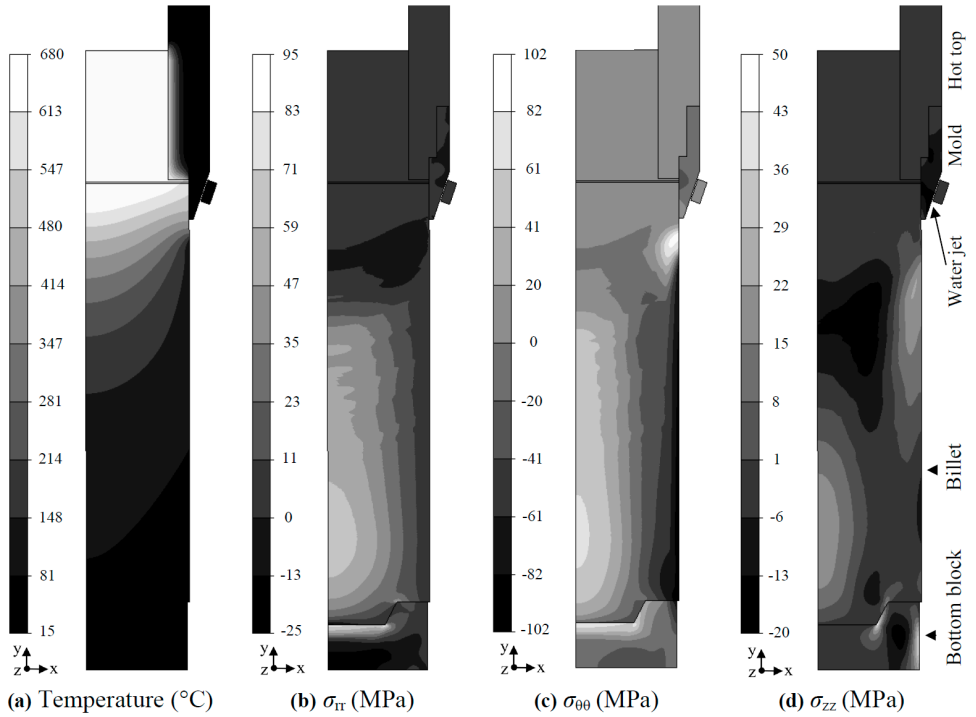

Fig.1 Computer simulation results showing the contour maps of: (a) temperature, and normal residual thermal stresses in b) radial, c) circumferential and d) axial direction after 380 s of casting at speed 1 mm/s.

To be able to discuss the failure probability in the billet the contour maps of the three components of the principal stress tensor ($\sigma_{33}<\sigma_{22}<\sigma_{11}$) are shown in Fig.2a, b, and c. In agreement with the results shown in Fig.1 the principal stress components appear to be tensile in the center of the billet and compressive at the surface. As discussed by Boender *et al.* [17], although having three tensile principal stress components in the center results in a nearly zero equivalent von Misses stress, it does not imply that no failure may occur. In other words, such a stress state facilitates the occurrence of a brittle fracture in the center of the billet. According to Rankine's theory which is more applicable to brittle materials, failure occurs when either the maximum principal stress reaches the tensile strength or the minimum principal component reaches the uniaxial compressive strength [18]. As the stresses computed by ALSIM are far below the tensile strength of the material (150 MPa at 200°C to 250 MPa at room temperature [11]), the effect of stress raisers (cracks and flaws) should be taken into account. Similarly, in a brittle material and under a triaxial state of stress cracks mainly orient themselves normal to the largest component of the principal stresses (σ_{11}) [19]. Hence, the maximum principal stress component was selected for calculation of the critical crack sizes. A penny shaped crack was

chosen as a 3D crack resembling the actual void shape in billets. For such a crack the critical crack size (radius of the penny) can be calculated as follows [20]:

$$a_c = \frac{\pi}{4}\left(\frac{K_{Ic}}{\sigma}\right)^2 \tag{1}$$

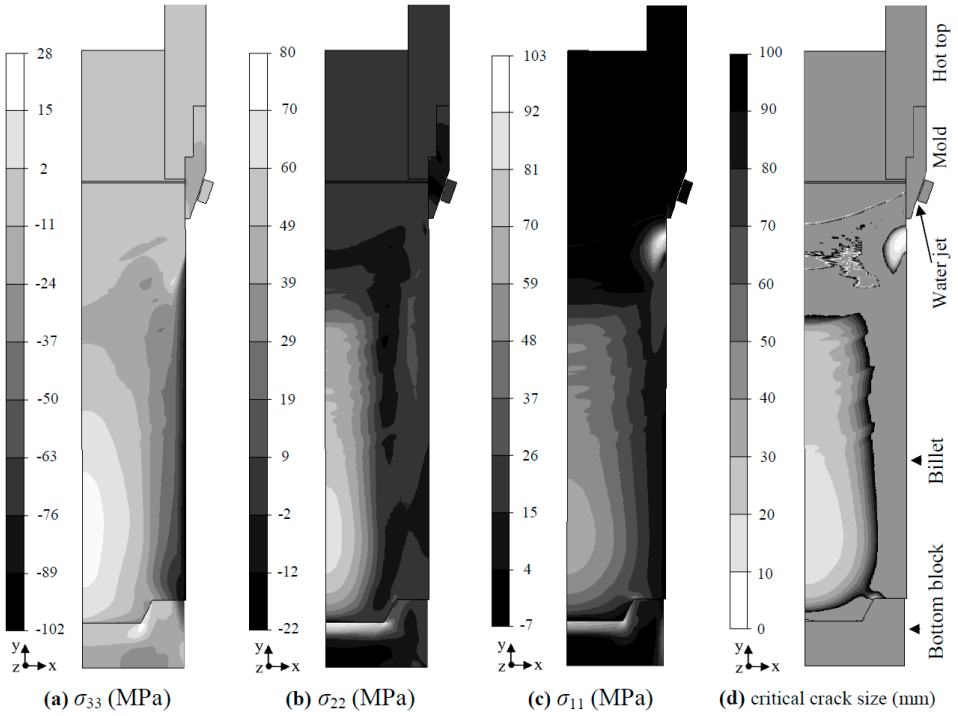

Fig.2 Computer simulation results showing the components of the principal stress tensor: (a) σ_{33}, (b) σ_{22}, and (c) σ_{11} after 380 s of casting at speed 1mm/s. (d) Critical crack size distribution for a penny shaped crack calculated using σ_{11}.

Fig. 2d shows the distribution of the critical crack size in a billet cast at a speed of 1 mm/s. As can be seen the most dangerous location appears to be in the WIZ where the critical crack size is below 10 mm. In the center of the billet the situation is the same although the critical crack size is larger due to smaller maximum principal stress values. Another vulnerable point is the corner on top of the bottom block. The cracking probability decreases by moving outwards from the center of the billet or the WIZ. In the remaining parts of the billet (mainly top center) stresses are either compressive or have low values resulting in unrealistic high values of critical crack size, which have been sorted out. Similar contour maps are shown in Fig. 3 for a billet cast at 2 mm/s. After 220 s, the stress state in the billet did not change noticeably. As can be seen, three components of the principal stress tensor (Figs. 3a, b, and c) have increased considerably compared to the case of 1 mm/s. A higher cast speed results in a higher heat input and eventually increases the temperature gradients especially in the "y" direction [21]. Fig. 3d shows the distribution of the critical crack size in the billet cast at 2 mm/s. Closer observation reveals two main differences with the billet cast at 1 mm/s. First, the critical crack size has decreased to below 10 mm in the center of the billet which is the result of higher maximum principal stress values there. The area with the smallest critical crack size is larger compared to the billet cast slower. Second, the area indicating the critical crack size in the WIZ has shrunk due to the shorter time the billet spends in this region. Although the direction of the principal stress components are not shown here, comparison of the stress tensor with the principal stress tensor revealed that the maximum principal stress is either in the radial or circumferential direction at lower cast speeds (1 mm/s). As the cracks propagate mainly normal to the largest component of the principal stresses, cracks with planes parallel to the axial direction of the billet result. At higher cast speeds (2 mm/s)

however, the maximum principal stress axis turns towards the axial direction of the billet, which in turn results in crack planes normal to that direction.

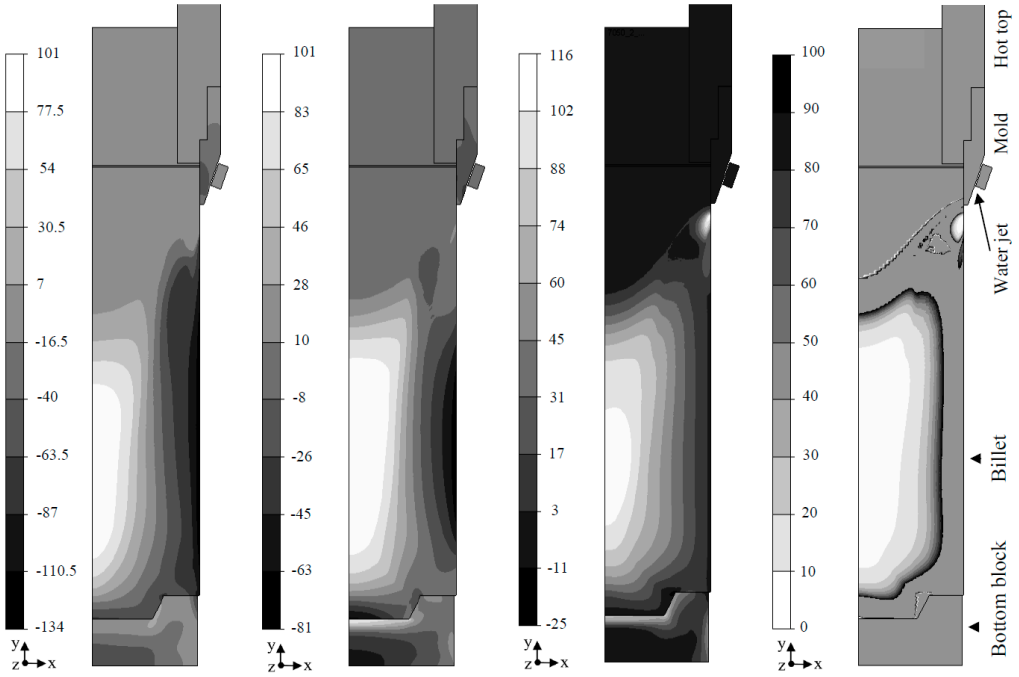

Fig.3 Computer simulation results showing the components of the principal stress tensor: (a) σ_{33}, (b) σ_{22}, and (c) σ_{11} after 220 s of casting at speed 2 mm/s. (d) Critical crack size distribution for a penny shaped crack calculated using σ_{11}.

4. Conclusions

Cold cracking propensity of the AA7050 alloy during DC-casting was studied using the computer simulated thermal stresses and the plane strain fracture toughness of the alloy in the genuine as-cast condition. Computer simulation results showed that the normal thermal stresses are all tensile in the center, while they either diminish or turn to compressive as we move towards the surface of the billet. The stress state at the surface passes through a transition from tensile to compressive as the billet leaves the water impingement zone. Therefore, the WIZ and the billet center appear to be the most vulnerable locations of the billet to cracking. Critical crack sizes leading to catastrophic failure were eventually calculated for a penny shaped crack using the maximum principal stress component in the billet and the corresponding K_{Ic} values. Cracking probability decreases with moving from the center towards the surface of the billet due to the decrease of the maximum principal stress value. The smallest critical crack size is observed in the WIZ, where the highest maximum principal stress is observed. In spite of this, billets rarely crack at the surface at lower casting speeds as tensile stresses are immediately replaced by compressive ones. Increasing the casting speed not only increases the magnitude of the maximum principal stress, but it also turns its axis towards the axial direction of the billet resulting in the rotation of the crack plane.

Acknowledgments

This research was carried out under the project number MC4.05237 in the framework of the Research Program of the Materials innovation institute M2i (www.m2i.nl). Support and fruitful discussions with Dr. W. Boender (Corus R&D) are appreciated. Another important basis of the present paper is

comments received from Messrs D. Mortensen and H. Fjær and Dr. A. Ten Cate. Authors would like to especially thank Dr. A. Ten Cate for the preparation of the geometry and mesh simulation files.

References

[1] J. Campbell: *Castings*, (Butterworth-Heinemann, Oxford (UK), 1991) pp.242-243.
[2] M. Lalpoor, D.G. Eskin and L. Katgerman: Mater. Sci. Eng. A 497 (2008) 186-194.
[3] T.W. Clyne and G.J. Davies: Br. Foundryman 74 (1981) 65-73, Br. Foundryman 68 (1975) 238-244.
[4] M. Rappaz, J.-M. Drezet and M. Gremaud: Metall. Mater. Trans. A 30 (1999) 449-455.
[5] D.J. Lahaie and M. Bouchard: Metall. Mater. Trans. B 32 (2001) 697-705.
[6] M. M'Hamdi, A. Mo and H.G. Fjær: Metall. Mater. Trans. A 37 (2006) 3069-3083.
[7] V.A. Livanov: *Aluminum Alloys*, Ed. by A.F. Belov and G.D. Agarkov, (Oborongiz, Moscow, 1955) pp.128-168.
[8] K. Matsuda, S. Nagai, Y. Miyate, H. Maehara and I. Tsukuda: *6th International Aluminum Extrusion Technology Seminar*, (Aluminium Association and Aluminium Extruder's Council, vol. I, Chicago, Illinois, USA, 1996) pp. 525-528.
[9] W. Boender and A. Burghardt: *5th Decennial Int. Conf. on Solidification Processing*, Ed. By H. Jones, (University of Sheffield, Sheffield (UK), 2007) pp. 714-718.
[10] O. Ludwig, J.-M. Drezet, B. Commet and B. Heinrich: *Modeling of Casting, Welding and Advanced Solidification Processes XI*, Ed. by C-A. Gandin and M. Bellet, (TMS, Warrendale (PA), 2006) pp.185-192.
[11] M. Lalpoor, D.G. Eskin and L. Katgerman: *12th Intern. Conf. on Fracture*, (National Research Council of Canada, Ottawa, 2009) (CD).
[12] M. Lalpoor, D.G. Eskin and L. Katgerman: Metall. Mater. Trans. A 40 (2009) 3304-3313.
[13] E.E. Madsen: *Numerical Methods in Thermal Problems*, Ed. by R.W. Lewis and K. Morgan, (Pineridge Press Limited, Swansea, United Kingdom, 1979) pp. 81-89.
[14] H. Fossheim and E.E. Madsen: *Light Metals*, Ed. by W.S. Peterson, (TMS-AIME, Warrendale,1979) pp. 695-720.
[15] E.K. Jensen and W. Schneider: *Light Metals*, Ed. By C. M. Bickert, (TMS-AIME, Warrendale, 1990) pp. 937-943.
[16] H.G. Fjær and A. Mo: Metall. Trans. B 21 (1990) 1049-1061.
[17] W. Boender, A. Burghardt, E.P. van Klaveren and J. Rabenberg: *Light Metals*, Ed. by A.T. Tabereaux (TMS, Warrendale, 2004) pp. 679-684.
[18] J.H. Faupel and F.E. Fisher: *Engineering Design*, (John Wiley & Sons, Inc., New York (NY), 1981) pp. 242-252.
[19] M. Schöllmann, H.A. Richard, G. Kullmer and M. Fulland: Int. J. Fracture 117 (2002) 129-141.
[20] H. Tada, P.C. Paris and G.R. Irwin: *The Stress Analysis of Cracks Handbook*, 3rd Ed., (ASME Press, New York (NY), 2000) p.342.
[21] J.F. Grandfield and P.T. McGlade: Materials Forum 20 (1996) 29-51.